PHYSICAL REVIEW A VOLUME 25, NUMBER 4 APRIL 1982

Absolute photoabsorption cross section of the K shell of atomic lithium

G. Mehlman,* J. W. Cooper, and E. B. Saloman
National Bureau of Standards, Washington, D.C. 20234
(Received 15 September 1981)

The absolute cross section of atomic lithium has been measured in the spectral range from 175 to 110 Å thus extending previous work to shorter wavelengths. Good agreement is found with theoretical predictions. The autoionizing-resonant-structure excitation between 176 and 160 Å has been measured and line-profile parameters obtained for several of the resonances. The resonant structure for core excitation associated with $N=3$ and $N=4$ principal quantum numbers is found to bear a close relationship to the analogous excitations in helium. A new classification of the resonant structure is given and comparisons made with theoretical results. A discussion of the total oscillator strength for K-shell excitation in lithium is given and the results obtained from the present and previous work are compared with the Thomas-Reiche-Kuhn sum-rule value.

I. INTRODUCTION

Studies on the absorption of atomic lithium were begun in this laboratory a number of years ago with the discovery of a complex resonant structure near the threshold for inner-shell excitation.[1] More recent work[2,3] has succeeded in providing absolute values for the cross section near the inner-shell-ionization threshold and, in addition, provided some information regarding the relative probability of leaving the ion core in various excited states following photoionization. The present paper is devoted to an extension of this work to shorter wavelengths. Coupled with previous work on photoabsorption above the first ionization threshold,[4] these results extend our knowledge of the photoabsorption of ground-state lithium to all energy regions where there is appreciable absorption.

The absorption from the ground state of lithium is of interest for several reasons. Absorption below the inner-shell-ionization threshold has been studied extensively[5] and agreement between theory[6] and experiment is excellent. More recently, theoretical calculations have been made[7,8] at higher energies corresponding to inner-shell ionization. These may be compared with the measurements reported here. Recently, there has also been considerable interest in the doubly excited states of lithium reached via core excitation as possible candidates for uv lasers.[9,10] This interest has led to studies of the doubly excited states of even parity, the principal candidates for such systems.[11,12] Further studies of the ground-state absorption in the region of double excitation should be useful both in interpreting these new experimental results and in providing more detailed information on the doubly excited states of odd parity.

The principal results of the present work are the following:

(1) The absolute-cross-section measurements reported previously have been extended from 172 to 110 Å.

(2) Details on the structure of the doubly excited resonances immediately below the $1s\,3l$ and $1s\,4l$ limits of the Li^+ ion are given.

(3) Resonance parameters for the first six resonances are obtained. A classification of the resonant structure is proposed and compared with theoretical results for $N=3$ and $N=4$ excitation in helium.

(4) With the use of the new data on the absorption cross section and previous results, the total oscillator strength for K excitation is estimated and compared with the value obtained from valence excitation data and the Thomas-Reiche-Kuhn sum rule.

(5) The results at short wavelengths are compared to previous measurements on solid lithium.

II. EXPERIMENTAL

Accurate absolute absorption cross sections are measured, as in previous work, utilizing the syn-

chrotron radiation continuum from the National Bureau of Standards storage ring (SURF II) and a grazing incidence scanning monochromator described previously.[13] This instrument, initially conceived for the purpose of making high-resolution cross-section studies in the photoionization continuum of atoms and molecules, provides a resolution of approximately 0.065 Å.

A heat pipe,[14] 83-cm long with resistive heating in the center and water cooling around both ends, is located in front of the monochromator entrance slit. The lithium column temperature profile was monitored by 12 thermocouples located at known positions 5 cm apart on the pipe's external wall. Helium was used as a buffer gas in the heat pipe because of its small cross section in the wavelength range of the experiment. The gas pressure used was always in the neighborhood of 1.5 Torr (200 Pa) and was monitored continuously during a spectral scan; it was measured with a calibrated capacitance manometer. Maximum temperatures at the center of the pipe were approximately 760 °C under these conditions. The temperature decreased by approximately 5% towards the ends of the pipe in the region where there was an appreciable density of lithium vapor. Temperatures in the buffer gas region at the ends of the pipe were typically several hundred degrees cooler. The lithium column length was found always to be close to 35 cm.

The light from the storage ring was focused through the heat pipe onto the monochromator entrance slit by an elliptical mirror at an 86° angle of incidence. The containment windows at each end of the heat pipe were beryllium foils about 2000-Å thick. For our observations between 110 and 200 Å (113–62 eV), the filtering of the background radiation by the beryllium windows minimized any stray light or second-order radiation.

The transmitted xuv (extreme ultraviolet) radiation was detected by a channeltron operating in a counting mode. The decrease of the storage ring output flux was correlated to the xuv count integration time period by monitoring the storage ring visible light emission. The monochromator was scanned at a variable speed correlated to the storage ring's visible output. Typical scanning speeds for high resolution in the region of the lithium resonances were of the order of 0.01 Å per 10 seconds. Standard pulse counting techniques were used in conjunction with a microcomputer data acquisition system. For the spectral range in the resonance region, the data points were taken at intervals of approximately 0.02 Å.

III. MEASUREMENT PROCEDURE

The process of data taking corresponds to several simultaneous measurements for each data point as follows: (1) Recording of the average channeltron position from which the wavelength is derived through the grating equation; (2) recording of the integrated number of counts corresponding to transmitted uv radiation over the wavelength interval scanned by the monochromator during a specified integration time; (3) recording of the count rate of the ring visible emission which in turn determines the integration time for the xuv transmitted flux as well as the scan speed of the monochromator; (4) recording of the buffer gas pressure; and (5) recording of the twelve thermocouple readings.

The values of the transmitted intensity $I(\lambda)$ were measured as a function of wavelength. Both before heating and after complete cooling of the heat pipe the instrument transmission of the incident intensity, $I_0(\lambda)$, was recorded over the same wavelength range with no gas present. The experimental data analysis was performed using a procedure which leads to a determination of the number density of lithium atoms and of helium atoms in the light path separately without a specific computation of the lithium column length X.

We shall outline here the basic steps of this analysis. The transmitted intensity through the heat pipe of length L at each wavelength λ, $I(\lambda)$ is related to the incident intensity $I_0(\lambda)$ by

$$I(\lambda)=I_0(\lambda)\exp\left[-\sigma_{\mathrm{He}}(\lambda)\int_0^L n(T)dl-\sigma_{\mathrm{Li}}(\lambda)\int_0^x N(T)dl\right], \quad (1)$$

where $\sigma_{\mathrm{He}}(\lambda)$ and $\sigma_{\mathrm{Li}}(\lambda)$ are the absorption cross sections for the buffer gas and the vapor, respectively, and n and N are the number densities of helium and lithium atoms, respectively. The total helium number density $\int_0^L n(T)dl$ was measured directly at wavelengths greater than the lithium $2\,^3S$ absorption threshold; i.e., where the lithium cross section is negligible and essentially all the absorption is due to helium. Thus, the total number density of helium atoms in the pipe's buffer gas region and transition zone can be obtained by measuring the intensity transmitted by the heat

pipe for wavelengths $\lambda' > \lambda_k$ where $\sigma_{He}(\lambda') >> \sigma_{Li}(\lambda')$. We measured $I(\lambda')$ for $\lambda_k = 210$ Å in a region where there is no helium structure; $I(\lambda')$ is given approximately by

$$I(\lambda') = I_0(\lambda') \exp\left[-\sigma_{He}(\lambda') \int_0^L n(T) dl\right] . \quad (2)$$

The helium cross section value was taken from the measurements of West and Marr.[15] Solving Eq. (2) for $\int_0^L n(T) dl$ and inserting this value in Eq. (1) we obtain the following relation:

$$\sigma_{Li}(\lambda) \int_0^x N(T) dl = \frac{\sigma_{He}(\lambda)}{\sigma_{He}(\lambda')} \ln \frac{I(\lambda')}{I_0(\lambda')} - \ln \frac{I(\lambda)}{I_0(\lambda)} . \quad (3)$$

The number density of lithium atoms in the light path is proportional to the quantity $(p/T)dl$ at each point along the pipe. Under proper operation the measured buffer gas pressure is in equilibrium with that of the lithium column. At each point including the transition zones the correct vapor pressure was obtained from the temperature readings using Nesmeyanov's empirical relation[16]:

$$\log_{10} p = 12.9992 - \frac{8442.53}{T} - 1.640\,38 \log_{10} T + 2.5968 \times 10^{-4} T , \quad (4)$$

where T is in degrees K, p in Torr, and log is in base 10. Interpolation between the thermocouple measurements provided the vapor pressure profile.

Thus, for each interval $\Delta l = 1$ cm of the pipe, the quantity $(p/T)\Delta l$ was computed and a summation over the whole vapor column yielded

$$\int_0^x N(T) dl \simeq 9.65 \times 10^{18} \sum \frac{p(l)}{T(l)} \Delta l . \quad (5)$$

The helium pressure was maintained as constant as possible. Maximum variations of about 0.1 Torr (6%) were recorded during a spectral scan including the measurements at $\lambda' > 210$ Å. Such pressure variations were taken into account in the computation of the absorber number densities. The lithium cross section at any wavelength was then obtained from Eqs. (3) and (5).

IV. ABSOLUTE CROSS-SECTION VALUES

The measured cross section σ obtained from a single scan between 175 and 115 Å is shown in Fig. 1. Selected values at indicated wavelengths are also shown in Table I. The recorded buffer gas pressure during this scan was in the vicinity of 1.4

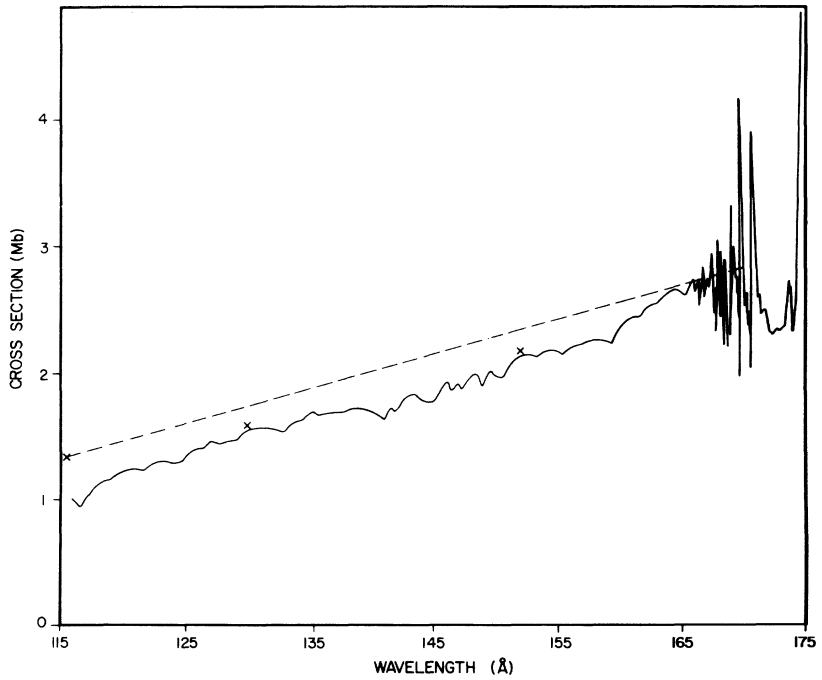

FIG. 1. The total photoabsorption cross section of lithium in the 115–175-Å region. – – –, theory, Ref. 8; ×, theory, Ref. 7.

Torr (186 Pa) corresponding to the vapor pressure of lithium at the recorded maximum temperature (760 °C). The number density in the light path varied slowly during this scan from 5.1×10^{17} to 4.7×10^{17} atoms/cm^3. Similar results are obtained from other scans at slightly different buffer gas pressures. Under these conditions the partial pressure of Li_2 molecules is about 3.5% of the total vapor pressure.[17] The cross-section values derived from our measurements have been corrected for this molecular contribution.

The value of the cross section obtained at wavelengths above 180 Å is of the order of 3 Mb, that is slightly larger than shown in Fig. 1 of Ref. 2. From repeated measurements of the instrument transmitted flux, we estimate the accuracy in the relative spectral distribution of the cross secton to be better than 10%. The major uncertainties in the absolute-cross-section determination are the uncertainty in the vapor pressure data of Ref. 16 and the possibility that the temperatures within the vapor column might be different than those measured at the exterior walls of the heat pipe. We estimate the absolute accuracy of the measurements to be approximately 20%. The dashed line in Fig. 1 corresponds to the theoretical values of the lithium cross section calculated by Reilman and Manson[8] using the Hartree-Slater central-field method; agreement is well within our experimental error. The three points plotted as "x" in Fig. 1 correspond to estimated values of the theoretical cross section curve from Fig. 4 of Amusia *et al.*[7]; they are in closer agreement with our experimental curve.

TABLE I. Total absorption cross section of lithium vapor between 70 and 100 eV.

Wavelength (Å)	Energy (eV)	Cross section (Mb)
180	68.9	2.8
172	72.1	2.4
165	75.1	2.7
160	77.5	2.4
150	82.6	2.1
140	88.6	1.75
130	95.4	1.6
120	103.3	1.22

V. RESONANT STRUCTURE IN THE WAVELENGTH RANGE 160–175 Å

A. Results

In addition to the resonant structure appearing in the wavelength region 211–180 Å which is associated with the $N=2$ states of the Li^+ ion, higher-lying resonances associated with the $N=3$ and $N=4$ states of Li^+ exist. The lowest of these resonances at 173.4 Å was reported in Ref. 1 and tentatively classified as $[1s(3s\,3p)^3P]^2P$. More recently the lithium absorption spectrum was photographed by Cantú *et al.*[18] in this spectral range and a tentative classification proposed.

As part of the present investigation, the spectral region between 175 and 150 Å has been examined in detail in order to provide more information on the higher energy resonant structure. The work reported here verifies earlier work in this laboratory[19] which provided a list of wavelengths corresponding to maxima in absorption in the 175–160-Å range from observations made photographically using the techniques of Ref. 1. The earlier work supplements the more recent measurements since the use of helium lines as wavelength standards provides an accurate wavelength scale. This could not be done in our measurements since data were taken for each run over a limited spectral range.

Tables II and III contain the results of both the previous work on the higher-lying resonant structure and the present work. Table II lists 17 resonances in the vicinity of the $N=3$ thresholds of Li^+. Twelve of these lie below the $(1s\,3s)^3S$ limit (167.154 Å) and the remaining five below the $(1s\,3s)^1S$ limit (166.034 Å) of Li^+. Six of these agree with the data of Ref. 18. Table IV contains the three observed resonances associated with $N=4$ excitation. All of these lie below the $(1s\,4s)^3S$ limit (160.39 Å). No other resonances appear in the data of the present experiment although the region out to 153.01 Å (the limit of double ionization of Li) was scanned with the same spacing as that used for the 160–175-Å region.

The first eight resonances corresponding to $N=3$ excitation are moderately well resolved and have asymmetric profiles as can be seen in Fig. 2. Parametric fits to these resonances were made using a method described previously.[20]

Briefly, the fitting procedure assumes that each resonance may be represented as a Beutler-Fano profile.[21] The resonance parameters E_0 (resonance energy), Γ (linewidth), q (asymmetry parameter),

TABLE II. Observed resonances in the neighborhood of the $N=3$ limits of Li^+. Wavelengths listed correspond to peaks in absorption. The classification is based on that of Ref. 24 for doubly excited resonances in helium. The notation $(N,\alpha)^{1,3}P$ identifies the resonances via principal quantum number $N(=3$ here), outer quantum number $n(\geq 3)$, and series label α. $[1s(N,n\alpha)^{1,3}P]^2P$ coupling is assumed. See text.

Wavelength (Å)	Observed Ref. 18 (Å)	Energy (eV)	Predicted energy (eV)	Classification
174.24	174.28	71.16	71.48	$(3,3a)^3P$
173.47		71.47	71.92	$(3,3a)^1P$
170.56		72.69	72.60	$(3,3b)^3P$
169.60	169.56	73.10	73.26	$(3,4c)^1P$
169.12	169.09	73.31	73.36	$(3,3b)^1P$
			73.43	$(3,4a)^3P$
168.83		73.44	73.45	$(3,4c)^3P$
168.33	168.31	73.65	73.67	$(3,4a)^1P$
167.99	167.99	73.80	73.76	$(3,4d)^1P$
167.79	167.77	73.89	73.95	$(3,4b)^3P$
167.60		73.98	74.00	$(3,4d)^3P$
			74.03	$(3,5c)^1P$
167.32		74.10	74.09	$(3,5a)^3P$
			74.14	$(3,5c)^3P$
167.18		74.16	74.19	$(3,4b)^1P$
	167.154	3^3S	limit	
166.90		74.29		
166.75		74.35		
166.66		74.40	unclassified	
166.51		74.45		
166.19		74.61		

and ρ (overlap parameter) were obtained for each resonance by deconvoluting the spectral response function, which was represented as a Gaussian with a full width at half maximum equal to the optical slit width of the monochromator (0.065 Å), via a least-squares procedure. Resonance parameters are shown in Table III. Note that the resonance positions obtained from this analysis differ

TABLE III. Profile analysis of the eight lowest $N=3$ resonances.

Classification	Wavelength (Å)	Energy[a] E_0 (eV)	q	Width Expt (eV)	Width Theory[b] (eV)	ρ	f[c]
$(3,3a)^3P$	174.24	71.14	−2.6	0.10	0.097	0.38	0.0034
$(3,3a)^1P$	173.47	71.47	−5.0	0.17	0.151	0.07	0.00072
$(3,3b)^3P$	170.56	72.71	−0.5	0.021	0.049	0.76	1.04×10^{-4}
$(3,4c)^1P$	169.60	73.12	−0.44	0.024	0.0028	0.82	1.07×10^{-4}
$(3,3b)^1P$	169.04	73.35	−0.35	0.087	0.068	0.4	5.8×10^{-5}
$(3,4c)^3P,(3,4a)^3P$	168.83	73.44	−0.14	0.043	0.023	0.57	9.4×10^{-6}
$(3,4a)^1P$	168.33	73.67	−0.37	0.019	0.047	0.54	2.6×10^{-5}
$(3,4a)^1P$	167.99	73.82	−0.26	0.08	0.0009	0.43	3.4×10^{-5}

[a]Note that the energies of these resonances differ slightly from that shown in Table II. The values here correspond to calculated resonance positions from the fit to the experimental data; those of Table II to peaks in absorption.
[b]Theoretical widths are from Ref. 26.
[c]f values are obtained from Eq. (6) of the text.

TABLE IV. Observed resonances in the neighborhood of the $N=4$ thresholds of Li^+.

Wavelength (Å)	Energy (eV)	Predicted energy (eV)	Classification
164.29	75.47	75.57	$(4s\,4p)^3P$
162.23	76.42	76.44	^1P
161.70	76.68		?

somewhat from the values of peak absorption shown in Table II. Also note that all of the resonances with the exception of the first two have rather small q values, although this is not obvious from the data presented in Fig. 2. The reason for this is that the background cross section at wavelengths shorter than 167 Å is high as is shown in Fig. 1.

B. Analysis of the $N=3$ and $N=4$ resonant structure

The autoionizing resonances near the $(1s\,2l)^{1,3}S,P$ thresholds of Li^+ have been discussed previously and a partial identification of the resonance structure has been made.[1] Of the six possible series of ^2P resonances that might be expected to converge to the four thresholds, only two could be identified as Rydberg series; i.e., the $[(1s\,2s)^3S\,np]^2P$ series which lies below the ^3S limit and the $[(1s\,2p)^1P\,ns]^2P$ series which, with the exception of the lowest member, lies above the ^3S limit. It was also pointed out in the previous work that the lowest members of these series should be classified as $[1s(2s\,2p)^3P]^2P$ and $[1s(2s\,2p)^1P]^2P$ in agreement with theoretical calculations.[22] The resonances between the ^3S and ^1P limits were the subject of a separate investigation[23] which showed that, owing to the strong coupling between the four channels and the large autoionization widths, only tentative classifications could be given to the complex structure between the $Li^+(1s2s)^3S$ and $(1s\,2p)^1P$ ionization limits.

The structure near the $N=3$ and $N=4$ limits is even more complex. One would expect ten series of resonances converging to the six limits for $N=3$, and fourteen series converging to the eight limits for $N=4$, respectively. An analysis of the

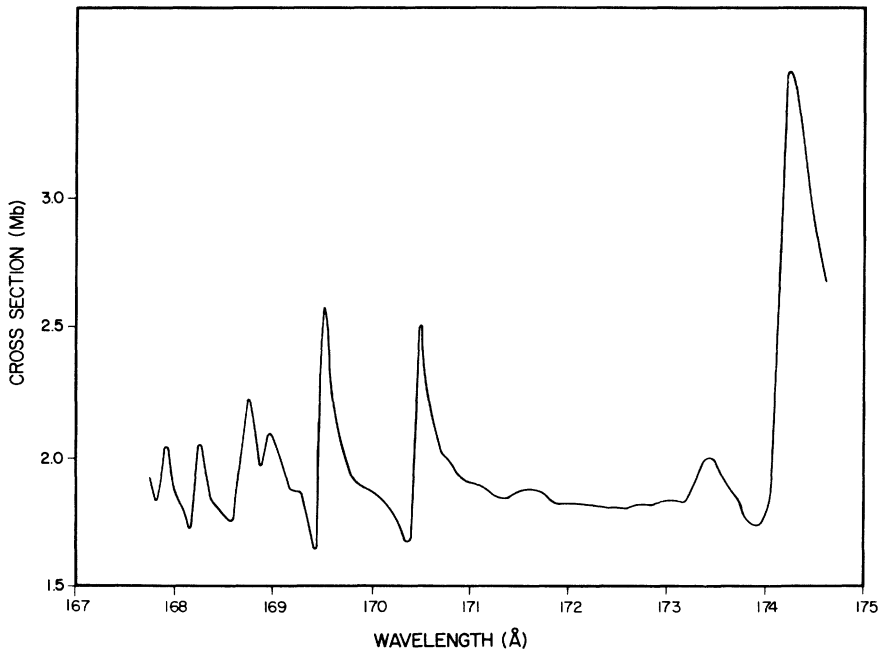

FIG. 2. The structure in the cross section in the region below the $3\,^3S$ threshold (167–175 Å).

data in Tables II and IV shows that there are no Rydberg series converging to any of the series limits. Nevertheless, a fairly successful classification of the observed $N=3$ and $N=4$ structures can be given based on their close analogy to the doubly excited resonances of helium.

The analogy is based on the following considerations. The resonances near the $N=3$ and $N=4$ thresholds are considered as doubly excited two-electron states coupled weakly to a $1s$ core electron. The physical picture is that of two electrons at large, but comparable, distances from the core which interact strongly with each other, but only weakly with the core electron. If the coupling to the core is completely negligible, the energy spacing of the resonances will be completely determined by the energy spacing of the states comprising the doubly excited two-electron configurations. Furthermore, the spacing of these states will be given to good approximation by the spacing of the doubly excited states in helium, since the core electron will provide almost complete screening of a single nuclear charge. For comparison with the resonances observed in absorption in lithium, only ^3P and ^1P doubly excited states need be considered, since they are the only states that can couple to the $1s$ core to form the ^2P states accessible in absorption from the ^2S ground state.

The core coupling, of course, is never completely negligible. However, some idea of its strength and of how useful the above ideas may be can be obtained by considering the lowest resonances of ^2P character which lie below the $2\,^3S$ and $3\,^3S$ thresholds. From Ref. 1, the two lowest ^2P resonances, $[1s(2s\,2p)^3P]^2P$ and $[1s(2s\,2p)^1P]^2P$, respectively, lie 4.85 eV apart. The comparable spacing of the $(2s\,2p)\,^3P$ and $(2s2p)\,^1P$ resonances in helium is 2.36 eV,[24] indicating that the interaction with the core is considerably different for the two lithium resonances. In contrast to this, for the two lowest-lying ^2P resonances of Table II, the energy spacing is only 0.31 eV, whereas the spacing of the two lowest lying ^3P and ^1P resonances below the $N=3$ threshold in helium is 0.44 eV, in moderately good agreement with the experimental spacing. We interpret this as evidence that the core interaction for the lowest doubly excited ^3P and ^1P resonances in lithium is approximately constant for the $N=3$ resonances, but not for those lying near the $N=2$ thresholds. The assumption that the interaction with the core remains approximately constant for the higher-lying resonances listed in Tables II and IV provides the basis for their classification.

Detailed information is available from theoretical calculations on the energy positions of the doubly excited states in helium.[24–29] However, in order to make a direct comparison with the data presented here an adjustment of their energy positions is necessary. Since the $N=3$ and $N=4$ resonances lie close to the limit for double ionization the most appropriate way to make this adjustment appears to be the following. The limit for double ionization of helium is 79.0069 eV (Ref. 28) above the ground state. The analogous limit for double ionization of lithium is 81.034 eV. In comparing energy positions it is assumed that these two thresholds must have the same energy. Therefore their difference, 2.028 eV, must be added to the energy-positions of the helium doubly excited states.

In Table II, the experimental energy positions of the observed resonances in lithium are compared with the doubly excited ^1P and ^3P resonances in helium corresponding to $N=3$ excitation which have been adjusted in energy as described above. The comparison shows that the energy spacing of the observed resonances below the $3\,^3S$ threshold is in moderately good agreement with the spacing of the helium doubly excited resonances; the major deviations occurring for the four lowest resonances.

In making the comparison shown in Table II, the energy positions of the doubly excited helium resonances of Lipsky *et al.*[24] have been used and a classification of the resonances as $1s[(N,n\alpha)^{1,3}P]^2P$ is proposed based on the classification scheme of that work. The notation $(N,n\alpha)^{1,3}P$ serves to uniquely identify each resonance by principal quantum number (N), outer quantum number (n), and series label (α). The series label is assigned on the basis of either approximately constant quantum defects or alternatively, on an analysis of the configuration mixing of the hydrogenic basis set used in performing the calculations.

In the rather extensive literature on doubly excited states of helium other classification schemes are used.[26,27,29,30] The scheme of Ref. 24 is used simply because that reference provides the most complete list of resonances for comparison with the data presented here. There appears to be little disagreement on the energy positions of the $N=3$ $^{1,3}P$ resonances. For example, Chung and Davis[31] have recently calculated the lowest eighteen $^{1,3}P$ $N=3$ resonances. Their values deviate from those shown in Table II, by at most 0.04 eV, well within the deviations of the comparisons made with the lithium resonances.

The comparisons made in Table II provide

unambiguous classifications of 8 of the 12 resonances lying below the $3\,^3S$ threshold. The resonance at 168.83 Å might be either $[1s(3,4a)\,^3P]^2P$ or $[1s(3,4c)\,^3P]^2P$ and the three highest-lying resonances at 167.60, 167.32, and 167.18 Å have alternative classifications as shown in the table. No attempt has been made to classify the five resonances lying above the $3\,^3S$ thresholds, since there are many doubly excited resonances of helium in this energy range.

The data in Table III provide some additional information that can be compared with theory. Herrick and Sinanoglu[26] have calculated the autoionization widths of all of the resonances shown in Table III, and these widths are compared with those derived by the fitting procedure. The calculated widths show good agreement with experiment only for the two lowest resonances. Moderate agreement is obtained (within a factor of ~ 2.5) with the other resonances with the exception of the two resonances at 169.60 and 167.99 Å which appear to have much larger widths than the calculated values. In order to provide some estimate of the relative strength of the resonances, oscillator strengths have been derived from the resonance parameters using the relation[32]

$$f = 9.109\times 10^{15}\sigma\rho^2 q^2 \frac{\pi\Gamma}{2} , \tag{6}$$

where σ is the background cross section (in cm^2) and Γ the width in eV. The values obtained are also shown in Table III, and provide a rough indication of the strength of the resonances. One would expect the strengths of the resonances based on ^3P doubly excited states to be larger than those based on ^1P states by the following argument. To the extent that the coupling scheme $1s[(N,n\alpha)^{1,3}P]^2P$ is valid for the resonances, the $1s$ core electron will not participate in the transition from the ground state. Thus it is appropriate to recouple the ground state as

$$1s^2 2s\,^2S = \tfrac{1}{2}[1s(1s\,2s)\,^1S]^2S + \frac{\sqrt{3}}{2}[1s(1s\,2s)\,^3S]^2S . \tag{7}$$

To the extent that the radial matrix elements for transitions to states of the same N, n, and α based on ^1P or ^3P parentage are equal, the recoupling of Eq. (7) would predict that the transition strengths of the ^3P resonances would be three times greater than those of ^1P parentage. The ratios from Table III are 4.7 for the $(3,3a)$ resonances and 1.8 for the $(3,3b)$ resonances, in moderate agreement with this prediction.

The resonances lying below the $4\,^3S$ threshold at 160.39 Å are more difficult to classify using the above procedure. Energy levels for the analogous ^1P and ^3P doubly excited states of helium are given by Oberoi[25] and for ^3P states only by Herrick and Sinanoglu.[26] The latter reference also gives autoionization widths for the ^3P resonances.

In Fig. 3 the absorption cross section below the $4\,^3S$ threshold is shown along with the predicted positions of resonances obtained from the data of Ref. 25.

Only three sharp absorption features appear in the experimental spectra. The resonance at 164.29 lies 0.21 Å (0.1 eV) below the predicted position of the lowest ^3P resonance and is thus classified as $4s\,4p\,^3P$. The next three calculated resonances do not appear as definite peaks but some evidence of their presence appears in the data. From Ref. 26 the width of the second lowest ^3P resonance is 0.07 eV (0.15 Å) which appears to be consistent with the broad feature in the data at 163.25 Å. The next observed resonance appears to be the third lowest ^1P resonance, although some evidence of structure appears at the predicted positions of the lowest two ^1P resonances. The highest-lying resonance at 161.70 Å cannot be classified unambiguously due to the large number of doubly excited resonances predicted to lie in this spectral region.

VI. SUM-RULE VALUES AND COMPARISON WITH THE CROSS SECTION FOR SOLID LITHIUM

From the curve shown in Fig. 1, we estimate the oscillator strength between 165 and 113 Å to be 0.54 ± 0.11. Between the $2\,^3S$ threshold and 165-Å the oscillator strength is estimated from the measurements reported previously[2] to be 0.26 ± 0.05. It is to be noted that the oscillator strengths reported in Ref. 2 for the two largest features at 191 and 174.3 Å were in error. The correct values are 0.035 and 0.004, respectively. For the region below the $2\,^3S$ threshold the oscillator strength corresponding to $N=2$ excitation is contained in the single Rydberg series converging to the $2\,^3S$ limit observed previously.[1] We estimate the oscillator strength of the series to be 0.48 ± 0.02 based on the calculations of the lowest members in Ref. 7 and the observed data for the higher series members. The total oscillator strength for K-shell excitation in the region up to 113 Å is thus 1.28 ± 0.12 where the errors are added quadratical-

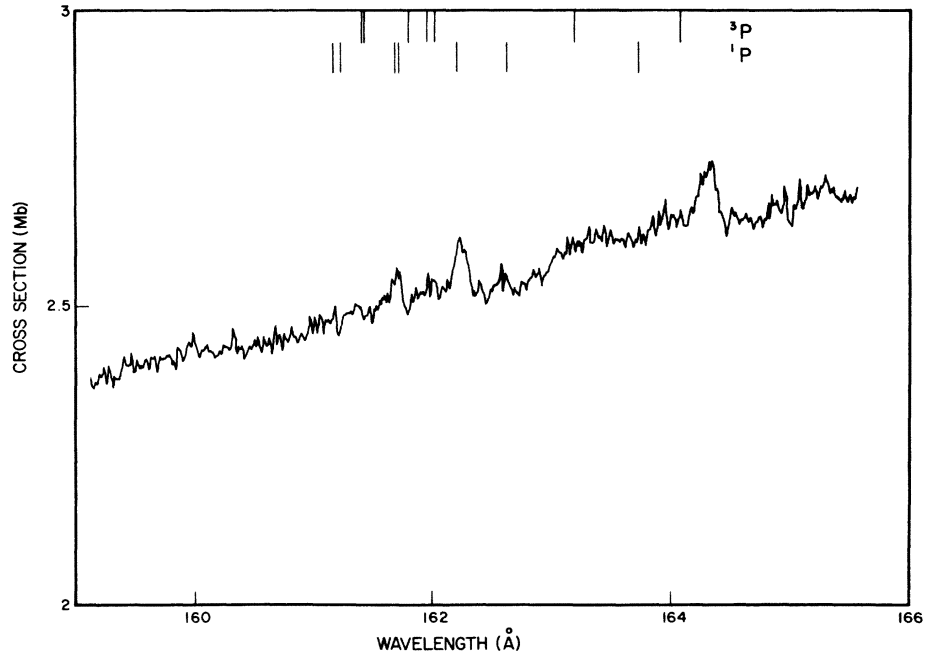

FIG. 3. The structure in the cross section in the region below the $4\,^3S$ threshold (159—166 Å). Predicted positions of ^3P and ^1P resonances obtained from Ref. 25 are shown at the top of the figure. See text.

ly. An integration of the theoretical curve of Ref. 8 in the region beyond 113 Å yields a value for the oscillator strength in the short wavelength region of 0.70 ± 0.05. This when added to the value above 113 Å yields a total oscillator strength of 1.98 ± 0.13. The total sum for valence excitation of lithium has been estimated to be 1.06,[33] thus all of the oscillator strength for ground-state excitation of lithium is accounted for. The close agreement of these numbers to integer values shows as expected that correlation between subshells has no major effect on the redistribution of oscillator strengths in lithium.[34]

In Fig. 4, the results of the measurements reported here have been extended beyond 100 eV by fitting the data at shorter wavelengths to the predicted $E^{-7/2}$ power-law dependence.[32] The extrapolated cross section curve has the same shape as that predicted by the numerical calculations.[7,8] Also shown are the results of a previous experiment on solid lithium.[35] Note that while the cross sections in this spectral region are comparable, the solid measurements have a different energy dependence than either the results obtained by extrapolating our data or by the theoretical predictions. The most likely cause of the discrepancy is the presence of some oxide contaminants in the previous measurements.[36]

VII. SUMMARY

Two key results have emerged from the work described in this paper. First, the absolute cross section for atomic lithium has been measured over

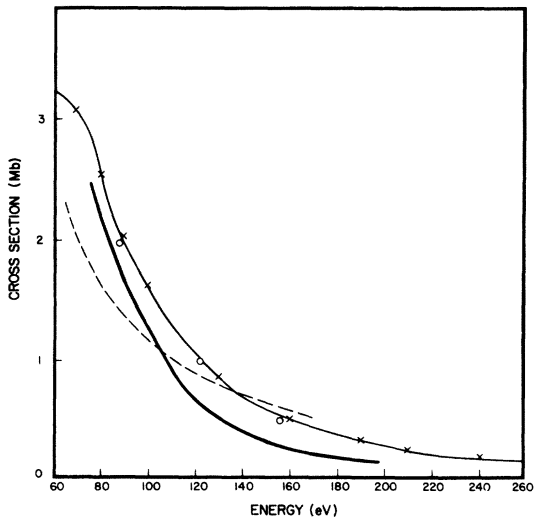

FIG. 4. Total absorption of lithium above 60 eV. ×, Ref. 8; ○, Ref. 7; — — —, absorption for thin-film measurements from Ref. 35; ——, present results (up to 107 eV) extrapolated to higher energies. See text.

an energy range sufficient to provide confidence in theoretical predictions in those spectral regions where autoionizing resonances do not make a major contribution to the cross section. Second, and possibly more important, some insight into the resonant structure for doubly excited states in lithium has been obtained which should be applicable to other atomic systems.

ACKNOWLEDGMENTS

This work would not have been possible without the dedicated work of staff of the Natl. Bur. Stand. (U.S.) SURF-II facility. Thanks are also extended to R. P. Madden, D. L. Ederer, and T. Lucatorto both for help while the work was being performed and for access to unpublished data.

---

*On leave from Laboratoire des Interactions Moléculaires et des Hautes Pressions Centre National de la Recherche Scientifique, Villetaneuse, France.

[1]D. L. Ederer, T. Lucatorto, and R. P. Madden, Phys. Rev. Lett. 25, 1537 (1970).
[2]G. Mehlman, D. L. Ederer, E. B. Saloman, and J. W. Cooper, J. Phys. B 11, L689 (1978).
[3]G. Mehlman, D. L. Ederer, E. B. Saloman, and J. W. Cooper, Jpn. Appl. Phys. Suppl. 17-2, 167 (1978).
[4]R. P. Hudson and V. L. Carter, J. Opt. Soc. Am. 57, 651 (1967).
[5]G. A. Martin and W. L. Wiese, Phys. Rev. A 13, 699 (1976).
[6]T. N. Chang and R. T. Poe, Phys. Rev. A 11, 191 (1975).
[7]M. Y. Amusia, N. A. Cherepkov, D. Zivanovic, and V. Radojevic, Phys. Rev. A 13, 1466 (1976).
[8]R. F. Reilman and S. T. Manson, Ap. J. Suppl. Ser. 40, 815 (1979).
[9]S. A. Mani, H. A. Hyman, and J. D. Daugherty, J. Appl. Phys. 47, 3099 (1976).
[10]S. E. Harris, Opt. Lett. 5, 1 (1980).
[11]T. J. McIlrath and T. B. Lucatorto, Phys. Rev. Lett. 38, 1390 (1977).
[12]J. R. Willison, R. W. Falcone, J. C. Wang, J. F. Young, and S. E. Harris, Phys. Rev. Lett. 44, 1128 (1980).
[13]R. P. Madden, D. L. Ederer, and K. Codling, Appl. Opt. 6, 31 (1964).
[14]C. R. Vidal and J. Cooper, J. Appl. Phys. 40, 3370 (1969).
[15]J. B. West and G. V. Marr. Proc. R. Soc. London, Ser. A 399, 397 (1976).
[16]A. N. Nesmeyanov, *Vapor Pressure of the Chemical Elements* (Elsevier, Amsterdam, 1963), p. 122.
[17]T. B. Douglas, L. F. Epstein, J. L. Denver, and W. H. Howland, J. Am. Chem. Soc. 77, 2144 (1955).
[18]A. M. Cantú, W. H. Parkinson, G. Tondello, and G. P. Tozzi, J. Opt. Soc. Am. 67, 1030 (1977).
[19]D. L. Ederer, T. Lucatorto, and R. P. Madden (private communication).
[20]D. L. Ederer, Appl. Opt. 8, 2315 (1969).
[21]U. Fano and J. W. Cooper, Phys. Rev. 137A, 1364 (1965).
[22]A. Weiss (private communication).
[23]J. W. Cooper, M. J. Conneely, K. Smith, and S. Ormonde, Phys. Rev. Lett. 25, 1540 (1970).
[24]L. Lipsky, R. Anania, and M. J. Conneely, At. Data Nucl. Data Tables 20, 127 (1977).
[25]R. S. Oberoi, J. Phys. B 5, 1120 (1972).
[26]D. R. Herrick and O. Sinanoglu, Phys. Rev. A 11, 97 (1975).
[27]K. T. Chung, Phys. Rev. A 6, 1809 (1972).
[28]W. C. Martin, J. Phys. Chem. Ref. Data 2, 257 (1973).
[29]J. W. Cooper, U. Fano, and F. Prats, Phys. Rev. Lett. 10, 518 (1963).
[30]J. Macek, J. Phys. B 1, 831 (1968).
[31]K. T. Chung and B. F. Davis, Phys. Rev. A 22, 835 (1980).
[32]U. Fano and J. W. Cooper, Rev. Mod. Phys. 40, 441 (1968).
[33]G. A. Martin and W. L. Wiese, Phys. Rev. A 13, 699 (1970).
[34]J. W. Cooper and J. B. Martin, Phys. Rev. 131, 1183 (1963).
[35]D. J. Baker and D. U. Tomboulian, Phys. Rev. 128, 677 (1962).
[36]D. L. Ederer (private communication).